

1 **Title:**

2 **HSC-independent definitive hematopoietic cells persist into adult life.**

3

4 Michihiro Kobayashi¹, Haichao Wei^{1,2}, Takashi Yamanashi⁴, David J Shih³, Nathalia Azevedo
5 Portilho¹, Samuel Cornelius¹, Noemi Valiente¹, Chika Nishida¹, Wenjin J Zheng³, Joonsoo Kang⁶,
6 Jun Seita^{4, 5}, Jia Qian Wu², Momoko Yoshimoto^{1*}

7

8 ¹Center for Stem Cell and Regenerative Medicine, Brown Institute of Molecular Medicine, and
9 ²The Vivian L. Smith Department of Neurosurgery, and ³Department of Dept. Biochemistry &
10 Molecular Biology, McGovern Medical School, University of Texas Health Science Center at
11 Houston, Texas, USA

12 ⁴Advanced Data Science Project, RIKEN Information R&D and Strategy Headquarters, Tokyo,
13 Japan

14 ⁵Center for Integrative Medical Sciences, RIKEN, Kanagawa, Japan

15 ⁶Department of Pathology, University of Massachusetts Medical School, Worcester, MA, USA

16

17 *Corresponding author

18 Momoko Yoshimoto MD., PhD

19 Momoko.Yoshimoto@uth.tmc.edu

20

21

22

23 **Summary**

24 The stem cell theory that all blood cells are derived from hematopoietic stem cell (HSC) is a
25 central dogma in hematology. However, various types of blood cells are already produced from
26 hemogenic endothelial cells (HECs) before the first HSCs appear at embryonic day (E)11 in the
27 mouse embryo. This early blood cell production from HECs, called HSC-independent
28 hematopoiesis, includes primitive and definitive erythromyeloid progenitors that transiently
29 support fetal blood homeostasis until HSC-derived hematopoiesis is established. Lymphoid
30 potential has traditionally been detected in the extra-embryonic yolk sac (YS) and/or embryos
31 before HSC emergence, but the actual presence of lymphoid progenitors at this stage remains
32 unknown. In addition, whether HSCs in the fetal liver are the main source of innate-like B-1a cells
33 has been controversial. Here, using complementary lineage tracing mouse models, we show that
34 HSC-independent multipotent progenitors (MPPs) and HSC-independent adoptive B-lymphoid
35 progenitors persist into adult life. Furthermore, HSCs minimally contribute to the peritoneal B-1a
36 cell pool; most B-1a cells are originated directly from ECs in the YS and embryo and HSC-
37 independent for life. Our discovery of extensive HSC-independent MPP and B-lymphoid
38 progenitors in adults attests to the complex blood developmental dynamics through embryo to
39 adult that underpin the immune system and challenges the paradigm of HSC theory in hematology.

40

41

42

43

44

45

46

47 **Introduction**

48 All blood cells are derived from special endothelial cells (ECs), referred to as hemogenic
49 endothelial cells (HECs) in the extraembryonic yolk sac (YS) and para-aortic region of the mouse
50 embryo during a limited time window^{1, 2, 3, 4, 5}. Before the emergence of hematopoietic stem cells
51 (HSCs) from HECs in the aortic regions at E11, multiple waves of blood cell production occur
52 directly from HECs, which contribute to the transient fetal hematopoiesis⁴. During this time, in
53 vitro B-lymphoid potential from HECs in the early YS and embryo has been reported^{6, 7, 8, 9},
54 however, the physiological presence of HSC-independent B-cells has yet to be unequivocally
55 determined. Furthermore, if they exist, how long and to what extent such HSC-independent B-
56 cells persist into postnatal life remains unknown. B-lymphocytes are mainly categorized into three
57 subsets; bone marrow (BM) HSC-derived B-2 cells (e.g., splenic follicular (FO) B-cells), marginal
58 zone (MZ) B-cells, and innate-like B-1 cells that reside mainly in the body cavities. CD5⁺ B-1a
59 cells are not replenished by BM HSCs and have generally been considered to be derived from FL
60 HSCs^{10, 11, 12} whereas contrasting results have also been reported^{13, 14}. In addition, it has been
61 reported that progenitors at E10.5 AGM region that have biased B-1 cell potential can acquire B-
62 2 potential upon AGM-derived endothelial niche culture¹⁴. Therefore, it is plausible that B-2 cells
63 may arise from HECs independently of HSCs.

64 In this study, using HSC- and EC-lineage tracing mouse models, we found that HSCs in
65 the FL slowly produced MPPs and B-lymphoid progenitors after birth and EC-derived HSC-
66 independent MPPs and B-progenitors persisted in adult for more than 6 months. Furthermore, FL
67 HSCs minimally contributed to the peritoneal B-1a cells and EC-derived HSC-independent B-1a
68 cells were the major population and maintained for life. Transplantation assays of E11.5 HSC-
69 precursors without co-culture demonstrated the presence of transplantable HSC-independent
70 MPPs and B-1a progenitors among this population. Our study resolved the long-lasting
71 controversy of B-1a cells and provide unexpected evidence of HSC-independent MPPs and
72 adaptive B-progenitors in adult life.

73 **Results**

74 *Fetal HSCs do not contribute to the peritoneal B-1a cell pool in a steady state.*

75 *Fgd5* is expressed exclusively in LT-HSCs [$\text{lin}^- \text{Sca-1}^+ \text{c-kit}^+$ (LSK)CD150⁺CD48⁻ cells] in the FL
76 and BM. *Fgd5CreERT2:Rosa-TdTomato (iFgd5)* mice enable us to label HSCs at a time of
77 Tamoxifen (TAM) injection^{15, 16}. We labeled HSCs in E14.5 FL or postnatal day 2 (P2) BM by TAM
78 injection, respectively, and examined Tomato% in various B-cell subsets and BM progenitors over
79 300 days after birth (Fig. 1A, B, Extended Date Fig. 1A, B). There were variations of Tomato
80 labeling efficiencies among animals and timed matings did not always precisely synchronize the
81 actual embryonic age at the time of TAM administration. Therefore, to evaluate the labeling
82 efficiency in a consistent manner, we calculated a Tomato % ratio of each blood cell type to HSCs
83 (Tomato % ratio =Tomato% of a defined cell type /Tomato% of HSC) as previously described¹⁶.
84 If a cell population is HSC-derived, Tomato % ratio should become close to 1.0 over time.¹⁶
85 Surprisingly, Tomato % ratio of B-1a cells stayed very low (<0.2) up to 300 days after birth (Fig.
86 1B) even when HSCs were labeled at E14.5 FL stage, indicating that the majority of adult
87 peritoneal B-1a cells were HSC-independent. Furthermore, the Tomato % ratios of MPPs and FO
88 B-cells showed 0.7-0.8 and 0.5, respectively (Fig. 1B, Extended Date Fig. 1A, B). This result
89 raised a question as to whether some of these cells in adults arise independently of HSCs.

90

91 *MPPs and B-progenitors in the FL are HSC-independent and originated at as early as E7.5.*

92 It has been reported that FL MPPs, but not LT-HSCs, produced B-1a cells most efficiently upon
93 transplantation^{13, 14}. Since fetal HSCs were not the major drivers of the peritoneal B-1a cells in
94 steady states (Fig. 1B), FL MPPs that have B-1a potential must be derived from precursors at
95 earlier stages than FL HSCs, such as HECs that can produce various hematopoietic cells^{17, 18}.
96 Therefore, we sought the origin of FL MPPs by using an EC-lineage tracing mouse model. *Cdh5*
97 is a specific marker of ECs and *Cdh5CreERT2: Rosa-TdTomato* mice (*iCdh5*) mice are widely
98 used to label ECs at a time of TAM injection¹⁹. First, we tried to label HECs that produce the first

99 de novo HSCs at E11.5. EC-labeling at E11.5 exclusively marked HSCs when we analyzed E15.5
100 FL (Fig. 1C, D). While $18.8 \pm 12.7\%$ of LT-HSCs were Tomato⁺, only $2.3 \pm 2.8\%$ of MPPs were
101 Tomato⁺, and its Tomato% ratio was only 0.1 (n=3) (Fig. 1D). These results indicate that even the
102 first HSCs produced at E11.5 do not yet differentiate into MPPs in the E15.5 FL, but gradually
103 produce MPPs and FO B-cells after birth (Fig. 1E). Additionally, B-1a cells were not efficiently
104 labeled by E11.5 TAM injection even when analyzed at >300 days (Fig. 1E, Extended Date Fig.
105 1C), in line with the HSC-lineage tracing results that HSCs do not produce B-1a cell efficiently.

106 Next, we sought the origin of FL HSC-independent MPPs at the earlier embryonic stages
107 before HSC emergence. We labeled ECs at E7.5 and examined Tomato⁺ MPPs and other
108 hematopoietic progenitors in E15.5 FL (Fig. 1F). Surprisingly, whereas LT-HSCs were barely
109 labeled, around 10-30% of MPPs were Tomato⁺ (Fig. 1G, Extended Date Fig. 1D). Furthermore,
110 other hematopoietic progenitors including common lymphoid progenitors (CLPs) and CD19⁺ B-
111 progenitors showed higher Tomato% than that of LT-HSCs (Fig. 1G, Extended Data Fig. 1D).
112 Because we labeled ECs, not HSCs, in *iCdh5* mice, the Tomato ratio=1.0 indicates that the target
113 cells and HSCs are derived from ECs at the same stage, and $\gg 1.0$ or $\ll 1.0$ indicates that these
114 two populations are derived from ECs at different time points²⁰. The Tomato % ratios of MPP,
115 CLP, and B progenitors to HSCs were much $\gg 1.0$ (Fig. 1G, H), indicating that E15.5 FL MPPs
116 and B-lymphoid progenitors were HSC-independent. Importantly, these HSC-independent MPPs
117 and B-progenitors marked at E7.5 persisted into adult life, more than 300 days after birth (Fig. 1H,
118 I).

119 When E9.5 ECs were labeled, the Tomato % of MPPs, other progenitors, and HSCs in the
120 E15.5 FL were similar (the ratio was near 1.0) (Extended Data Fig.1E). Considering that HSCs
121 expand rather than differentiate during E10.5 to E15.5^{21, 22}, this result suggests that most
122 progenitors and HSCs were simultaneously produced from HECs at E9.5. Importantly, these E7.5
123 and 9.5 HSC-independent MPPs persisted more than 300 days after birth because their tomato

124 ratio kept >1.0, suggesting that HSC-independent MPP-derived hematopoiesis occurs even in the
125 adult BM (Fig. 1H, I, Extended Data Fig. 1F).

126

127 *FL MPPs contain HSC-independent common B-1 and B-2 progenitors*

128 As Tomato⁺E15.5 FL MPPs are HSC-independent (Fig. 1G) and contain B-1a precursors upon
129 transplantation¹⁴, we examined their B-1 and B-2 progenitor potential using modified B-cell colony
130 assays¹⁴. From 500 Tom⁺ MPPs marked at E7.5 in *iCdh5* mice, 29 B-progenitor colonies were
131 detected (Extended Data Fig. 1G). Among them, we found 20 B-1 progenitor colonies and 9 B-1
132 and B-2 progenitor mixed colonies. These data showed that E15.5 FL HSC-independent MPPs
133 contain B-1 progenitors and common lymphoid progenitors that can differentiate into both B-1 and
134 B-2 cells.

135

136 *Most B-1a cells are derived from E7.5-10.5 HECs.*

137 Since HSCs after E11.5 showed minimal contribution to the peritoneal B-1a cells (Fig. 1E),
138 we examined at which stage of HECs mark the peritoneal B-1a cells most efficiently. We expected
139 that B-1a cells were derived from ECs at early embryonic stages similar to brain macrophage
140 (Extended Data Fig. 1H)²⁰. However, B-1a cells were marked by ECs during E7.5 to E10.5
141 (Extended Data Fig. 2, 3). Other B-cell subsets including FO and MZ B cells showed similar
142 labeling patterns (Extended Data Fig. 2, 3). Tomato% ratios of these B-1a and B-2 cells to HSCs
143 were just slightly higher than 1.0 when ECs were labeled at E7.5 or E8.5 (Fig. 1I, J). When E10.5
144 ECs were labeled, almost all B-lymphoid subsets including B-1a cells showed similar Tom % with
145 that of HSCs (the ratio of nearly 1.0) (Fig. 1K). These results suggest that B-1a cells, a part of
146 other B-cell subsets, and HSCs were produced simultaneously from ECs because HSCs after
147 E11.5 contributed to only a part of each B-cell subset (Fig. 1E, Extended Data Fig. 1C). Taken
148 together, the data indicate that most B-1a cells are derived from ECs during E7.5 to 10.5, and a
149 portion of FO and Marginal zone B-cells are also HSC-independent.

150 In order to explain the results from the *iCdh5* mouse (Fig. 1I-K, Extended Data Fig. 1C),
151 we constructed a mathematical model of label tracing experiments by extending a previously
152 established model²³. We constructed three variants of the label tracing model based on competing
153 hypotheses for the cell differentiation tree (Extended Data Fig. 4A). The base model M_0 assumes
154 a linear differentiation path from hemogenic EC via HSC, MPP, B-1 progenitor, and finally to B-1
155 cell. The M_1 model hypothesizes that ECs can directly differentiate into MPPs. In addition to M_1
156 model, the M_2 model hypothesizes that ECs can directly differentiate into B-1 progenitors. After
157 model fitting, the M_2 model yielded label tracing predictions that most closely resemble the
158 experimental label tracing data from the *iCdh5* mouse (Fig. 1I-K, Extended Data Fig. 1C, 4, 5).
159 These results indicate that the differentiation tree of the M_2 model can best explain the
160 experimental data, providing additional support that ECs directly differentiate into MPPs and B-1
161 progenitors independently of HSCs during fetal development.

162

163 *Single cell-RNA-sequencing showed heterogeneity and B-lymphoid signatures of pre-HSC and*
164 *HSC population*

165 Lineage tracing studies demonstrated the multiple waves of HSC-independent
166 hematopoiesis including MPPs, B-progenitors, and B-1a cells. We recently reported that E10.5
167 HSC-precursor (pre-HSC) population shows B-1 biased repopulating ability¹⁴. Pre-HSCs are
168 intermediate precursors between HECs and adult repopulating HSCs detected during E10.5 to
169 11.5 and express VE-cadherin (VC), encoded by *Cdh5*²⁴. At E11.5, the first adult repopulating
170 HSCs are detected²⁴. To understand the transition from pre-HSCs to HSCs or MPP, and their
171 heterogeneity of hematopoietic capability, we performed single-cell (sc) RNA-sequencing of
172 E11.5 AGM and YS VC⁺c-kit⁺EPCR⁺ pre-HSC population, E12.5 FL HSC (CD45⁺LSK⁺EPCR⁺)
173 and E14.5 FL HSCs (CD45⁺LSK⁺CD150⁺CD48⁻) (Extended Data Fig. 6). In parallel, selected
174 sorted subsets were transplanted into sublethally irradiated NSG neonates to validate their
175 hematopoietic capabilities (Extended Data Fig. 6D).

176 We sorted individual cells from above populations and generated single-cell full length
177 transcriptome using SMART-seq. We distributed the genes (read counts >10) in each cell and
178 excluded the cells which expressed less than 2000 genes and genes that were detected in less
179 than 10 cells (Extended Data Fig. 6E). At last, 95 cells and 11,814 genes were used for further
180 analysis. PCA analysis of scRNA-seq showed clear separation of FL HSCs from pre-HSCs (Fig.
181 2A). Notch-related genes were all highly expressed in many AGM cells but were downregulated
182 in FL HSCs (Extended Data Fig. 7) as previously reported transitional requirement of Notch
183 signaling²⁵. Unbiased sc consensus clustering (SC3) of the whole transcriptomes separated these
184 cells into four distinct clusters (Fig. 2B). The top 10 differentially expressed genes are depicted
185 in Extended Data Fig. 8. We focused the expressions of HSC- and lymphoid cell-related genes in
186 each cell (Fig. 2C) and examined the trajectory of cell states with ordering of cells from E11.5
187 AGM to E14.5 FL HSCs (Extended Data Fig. 9) using pseudo-time analysis. Trajectory map
188 indicated the progression of E11.5 AGM pre-HSCs to E12.5 and E14.5 FL HSCs (Extended Data
189 Fig. 9). Almost all pre-HSCs and HSCs expressed essential genes for B-cell development, such
190 as *Ikz1* and *Tcf3* in addition to many HSC-related genes (Fig. 2C, Extended Data Fig. 9). *Bcl11a*,
191 important for fetal and adult B cell development and globulin switching, is also widely expressed
192 among pre-HSCs and HSCs (Fig. 2C, Extended Data Fig. 9). Interestingly, essential BCR
193 signaling related genes, such as *CD79b* and *Btk*, were heterogeneously expressed in all cell types,
194 even in FL HSCs, suggesting their biased B-lymphoid potential (Fig. 2C, Extended Data Fig. 9).
195 *Lin28b*, encoding RNA-binding protein and critically important for B-1a cell generation^{11, 26}, is also
196 heterogeneously expressed among pre-HSC and HSC populations (Extended Data Fig. 9), which
197 may explain the contrasting results of FL HSCs transplantation assays^{11, 12, 13, 14, 27}. *Pbx1*, the Hox
198 cofactor and proto-oncogene, is essential for B-lymphoid lineage commitment and HSC-self-
199 renewal/maintenance^{28, 29, 30}. While *Pbx1* was widely expressed among pre-HSCs, its expression
200 was only seen in a small portion of HSCs (Fig. 2C, Extended Data Fig. 9). These data displayed
201 the heterogeneity of highly purified pre-HSC and HSC populations and even genes that have

202 been considered critical for HSC maintenance may not be expressed ubiquitously in FL HSCs.
203 We also performed the velocity analysis^{31, 32} to understand the gene expression status of each
204 cell. Interestingly, the velocity analysis showed two directions of the gene expression status into
205 the left and the right shown in Fig. 2D. When we compared the gene expressions between the
206 cells on the left and right sides, 41 genes were differentially expressed (supplementary file). We
207 examined these gene expressions in BM HSPC and B-progenitors from the database at ImmGen
208 (Fig. 2E) and found the difference of these gene expressions reflected the ones found in BM B-
209 progenitors or HSPCs. This result suggests that there may be divergence into HSC and B-cell
210 commitment of pre-HSC and HSC populations.

211

212 *HSC-independent MPPs and B-1 biased repopulating cells are present in E11.5 Embryo.*

213 Upon the heterogenous gene expression signatures of HSPC and B-cell lineages in pre-
214 HSC population, we examined the presence of HSC-independent MPPs and B-1a precursors in
215 the pre-HSC population in transplantation settings. We injected 5 -10 cells of CD45⁺Ter119⁻VC⁺c-
216 kit⁺EPCR⁺ pre-HSC population isolated from E11.5 aorta-gonad-mesonephros (AGM) region
217 (Extended Data Fig. 6A) into sublethally irradiated NSG neonates. Of total 25 recipient mice, 15
218 showed donor-derived CD45.2⁺ cells (>0.1%) in the peripheral blood (PB) (Fig. 3A). When we
219 analyzed the transplanted mice at 4-6 months post transplantation (Fig. 3B-D), we found there
220 were four types of engraftment patterns; multi-lineage engraftment including BM LSK cells (HSC-
221 engraftment, Fig. 3B-D, E-G, mouse #1-5); multi-lineage engraftment without BM LSK cells (MPP
222 engraftment, Fig. 3B-D, H, I, J mouse #6-11); and only B-1 and B-2 cell engraftment (Fig. 3B, C,
223 mouse #12); and only B-1 cell engraftment (Fig. 3B, C, K, mouse #13-15).

224 Mice #1-5 showed long-term multi-lineage repopulation with significant donor cell % in the
225 PB, peritoneal cavity, spleen, and BM (Fig. 3A-E) and predominant B-2 cell engraftment with B-
226 1a and B-1b cells (Fig. 3B). In the recipient BM, successful donor derived LSK cell repopulation
227 was also confirmed (Fig. 3F). Thus, these mice were categorized as HSC-repopulated mice.

228 Importantly, the secondary recipient BM also showed donor-derived LSK repopulation (Fig. 3G),
229 indicating that LSK-repopulating cells are the functional HSCs that harbor a self-renewal ability.
230 In contrast, mouse #6-11 showed long-term reconstitution without donor-LSK cells in the BM (Fig.
231 3A-D, H, I, J), indicating that they were engrafted with HSC-independent progenitors, thus named
232 MPP-engrafted mice. These mice showed predominant B-1 and MZ B cell engraftment with
233 seemingly diminishing B-2 cells in the peritoneal cavity and spleen (Fig. 3B, C) and B-2, T, and
234 myeloid cell engraftment in the PB and BM (Fig. 3D, H, I, J), although the donor percentage in
235 the BM was very low (<0.5%) (Fig. 3D, J). Mouse #13-15 showed B-1a, B-1b, and MZ B-cell
236 engraftment in the peritoneal cavity and spleen but did not show donor-derived cells in the BM
237 (Fig. 3B-D), indicating HSC-independent B-1 cell engraftment. One mouse (#12) showed only B-
238 1 and B-2 cell engraftment (Fig. 3B-D, K), suggesting the presence of common B-1 and B-2
239 progenitors.

240 These results strongly indicate that HSC-independent long-term engraftable MPPs and
241 B-1 precursors are present in E11.5 AGM region, also in line with the scRNA-seq data showing
242 the heterogeneity of these cells. Importantly, all engrafted mice showed B-1a cell repopulation
243 whereas B-2 cells were dominant in HSC-engrafted mice; thus, it seems that B-1a potential is the
244 default within E11.5 pre-HSCs and B-2 cell dominant capacity is a hallmark of functional HSCs.

245

246 **Discussion**

247 We demonstrated that definitive hematopoietic cells including MPPs, all B-cell subsets, and HSCs
248 are independently produced from HECs and persist into adult life. While HSC-independent B-1a
249 cells are rarely replaced by HSC-derived cells, HSC-independent MPPs and B-2 cells are
250 gradually replaced by HSC-derived cells. These findings challenge the current paradigm of HSC-
251 derived hematopoiesis and finally clarified the longstanding unresolved question regarding the
252 origin and main source of B-1a cells.

253 In adult murine hematopoiesis, it has recently been reported that MPP is a main driver of
254 native hematopoiesis and the discrepancy of HSC- and MPP-derived clones have been
255 observed³³. Our results explain this discrepancy, where the majority of MPPs in young mice are
256 HSC-independent, derived from fetal ECs, and HSC-derived hematopoiesis appears later, This
257 is also in line with the previous report that postnatal HSC-labeling showed gradual increase of
258 HSC-derived-lymphocytes over 32 weeks^{16, 23, 34, 35} and a recent report showing minimal
259 contribution of definitive HSCs to fetal hematopoiesis in a fish model³⁶. In addition, the presence
260 of HSC-independent MPPs in the pre-HSC population has also been reported using AGM-EC co-
261 culture system¹⁸. Therefore, together with our results, pre-HSC population is essential not only
262 for maturing to HSCs but also containing MPPs that support hematopoiesis in postnatal life.

263 Our lineage tracing results (Fig. 4A), difficult to reconcile with the current classic model
264 (Fig. 4B), instead lead us to propose a multiple hematopoietic wave model (Fig. 4C). In the current
265 classical model (Fig. 4B), YS-derived EMPs maintain hematopoietic homeostasis until perinatal
266 periods³⁷. Once HSCs are produced in the embryo, HSCs expand in the FL, start HSC-derived
267 hematopoiesis, and migrate to the BM just before birth, where HSCs maintain hematopoiesis for
268 life. Our model proposes that multiple waves of HSC-independent hematopoiesis, including EMP,
269 B-1 precursor and MPP production, occur from ECs, and persist into adult life. HSCs are also
270 produced as the final wave of EC-derived blood production. While HSCs expand in the FL, HSC-
271 derived hematopoiesis seems to first start after settling the BM, and gradually replaces the HSC-
272 independent hematopoietic cells over time. B-1a precursors are produced directly from ECs or
273 via HSC-independent MPPs at early- and mid-gestation but not replaced by HSC-derived cells in
274 steady state.

275 There are some discrepancies between lineage tracing study and transplantation assays
276 regarding the B-1a cell potential. While E11.5 EC labeling did not mark B-1a cells, E11.5 VC⁺ pre-
277 HSCs showed B-1a repopulating ability. This may be due to the difference of expression timings
278 of Cdh5 transcriptome and VC surface protein. In addition, the first HSCs at E11.5 possess B-1a

279 repopulating ability upon transplantation whereas FL HSCs did not. Therefore, HSCs may have
280 B-1a cell potential within a limited time window in transplantation or stress settings.

281 Taken together, we unveiled unappreciated presence of HSC-independent hematopoietic
282 progenitors in adult life and challenge the paradigm of HSC-dogma in hematology.

283

284 **Acknowledgement**

285 The scRNA-sequencing work was performed at the Single Cell Genomics Core at BCM partially
286 supported by NIH shared instrument grants (S10OD023469, S10OD025240) and
287 P30EY002520. This work is supported by NIH R01AI121197 (M.Y.), R01AI147685 (J. K.). H. W.
288 and J. Q. W. are supported by grants from the National Institutes of Health R01 NS088353
289 and R21 NS113068-01. This work was also partly supported by the National Institutes of Health
290 (NIH) through grants 1UL1TR003167 and the Cancer Prevention and Research Institute of Texas
291 through grant RP170668 (W.J.Z).

292 Some figures were created with BioRender.com.

293

294 **Data availability**

295 Sequencing data have been deposited in the GEO database under accession number
296 GSE182206.

297 All original code has been deposited at github and is publicly available as of the date of publication.

298 URLs are listed in the key resources table.

299

300 **Author contributions**

301 M.K. conceived, design, and performed experiments and analyzed the results. H.W., T.Y., J.S.
302 and J.Q.W participated in bioinformatics data analysis. D.J.S and W.J.Z calculated the
303 mathematical model, N.A.P., S.C., N.V., C.N. performed experiments, J.K. analyzed the results
304 and edited the manuscript, M.Y. conceived, design, and performed experiments, analyzed the
305 results, wrote and edited the manuscript.

306

307 **Methods**

308 ***Experimental Animals***

309 Cdh5(PAC)-CreERT2 mice were obtained from Dr. Ralf Adams. Fgd5CreERT2 mice (Stock No:
310 027789) and Rosa-TdTomato mice (Stock No: 007909) were obtained from Jackson Laboratory.
311 Cdh5(PAC)-CreERT2 mice were crossed with Rosa-TdTomato mice and Cdh5CreE2:Rosa-
312 Tomato mice were generated. Similarly, Fgd5CreERT2 mice were crossed with Rosa-TdTomato
313 mice and Fgd5CreERT2:Rosa-Tomato mice were generated. These mice were timed mated with
314 Rosa-Tomato mice and the vaginal plugs were confirmed in the following morning. The noon on
315 the day that the plug was found was counted as embryonic day 0.5. Tamoxifen (15ng/mother
316 body weight) was administrated into timed mated pregnant iCdh5 dams at E7.5, 8.5, 9.5, 10.5,
317 11.5 respectively, or into timed mated pregnant Fgd5 dams at E14.5, or P2 neonates. 10-15 mice
318 for each Tam injection date were examined.

319
320 For transplantation assays, C57BL/6 mice were timed mated and embryos at E11.5 were
321 harvested from the pregnant dams. AGM region was dissected from the embryo and lin-CD144+c-
322 kit+EPCR+ cells were sorted for donor cells. The embryonic age was confirmed by the somite
323 numbers and developmental features of the embryos.

324 NOD/SCID/Il2 γ ^{null} mice (NSG mice. Jackson Laboratory Stock No: 005557, OD.Cg-
325 *Prkdc*^{scid} *Il2rg*^{tm1Wjl}/SzJ mice) were timed mated and day2-5 neonates were used for recipients of
326 transplantation assays. Recipient NSG neonates were sublethally irradiated (150rad) before
327 donor cells were injected into facial vein. For secondary transplantation, 1-2 million BM cells from
328 the primary recipient mice were injected into lethally irradiated adult BoyJ mice.

329 Mice were kept in specific pathogen free condition and all the experimental procedures using the
330 mice were approved by Animal Welfare Committee at UTHealth.

331

332 ***Lineage tracing experiments***

333 Cdh5CreERT2:Tosa-Tomato mice were timed mated. A single dose of Tamoxifen (TAM)(Sigma)
334 15ng/mother body weight together with Progesterone (7.5ng/mother body weight) solved in corn
335 oil was administrated to the pregnant dam by oral gavage at E7.5, 8.5, 9.5, 10.5, and 11.5
336 respectively. TAM usually makes the delivery difficult, therefore, Cesarean section was performed
337 on day 19 pregnant dams to rescue the embryos and these pups were taken care of a surrogate
338 mother prepared in advance. Fgd5CreERT2: Rosa-Tomato mice were used for marking HSCs,
339 therefore, TAM was injected into E14.5 pregnant dam or P2 neonatal mice. We harvested various
340 hematopoietic tissues including peritoneal cells, spleen, thymus, and bone marrow from TAM
341 administrated embryos/mice and examined Tomato⁺ percentages in each hematopoietic subset.
342 We compared relative Tomato⁺ percentage between the cell population of interest and HSCs.
343 The surface markers used for flow cytometry is listed in the table.

344

345 ***Mathematical modeling of label tracing data***

346 We extended a previously established mathematical model for label tracing data²³. Consider
347 three successive cell compartments in hematopoiesis: upstream u , reference r , and
348 downstream d . For example, in the differentiation path HEC \rightarrow HSC \rightarrow MPP, compartment u
349 represents hemogenic EC, compartment r represents HSC, and compartment u represent
350 MPP. The change in cell number N_r over time t is given by:

351

$$352 \quad \frac{dN_r}{dt} = \beta_r N_r + \alpha_{u,r} N_u - \alpha_{r,d} N_r$$

353

354 where β_r is the net proliferation rate, $\alpha_{u,r}$ is the differentiation rate from compartment u to r , and
355 similarly for $\alpha_{r,d}$. Solving this differentiation equation leads to an exponential growth model for
356 N_r (when differentiation rates are set to zero). Biologically, over the lifetime of an organism, a

357 logistic growth model may be more realistic because each cell type would have an upper limit
358 on population size. We therefore modify the label tracing model as follows:

359

$$360 \quad \frac{dN_r^l}{dt} = \beta_r \left(1 - \frac{\sum_l N_r^l}{\kappa_r} \right) N_r^l + \alpha_{u,r} N_u^l - \alpha_{r,d} N_r^l$$

361

362 which imposes a carrying capacity κ_r that modulates the net proliferation rate. Integer l indexes
363 the cell number N_r in order to distinguish label compartments (Tomato⁻ vs. Tomato⁺). The label
364 compartments share the same parameters ($\beta_r, \alpha_{u,r}, \alpha_{r,d}$), because these parameters depend on
365 the cell type and are independent of label status. Conversely, both label compartments
366 simultaneously experience a common population limit, because the proliferation rate is
367 determined by the total cell number $\sum_l N_r^l$ marginalized over label status, as shown in the above
368 equation.

369

370 We implemented discrete-time simulations for label tracing models with various differentiation
371 trees (M_0, M_1, M_2) in the R environment (v4.1.1). The κ parameters were initialized to steady-
372 state compartment sizes that were previously determined whenever available (Busch et al.,
373 2015). The simulation models were used to predict cell numbers across time for each cell type
374 and label compartment, from which the label proportions and label ratios were calculated. The
375 model parameters were tuned so that the predicted label ratios resemble the experimentally
376 determined Td-Tomato label ratios.

377

378 ***B-progenitor colony forming assay***

379 Five hundred FL MPPs were plated to methylcellulose containing 10ng/ml IL-7 with 10^5 OP-9 cells.
380 Eight days after plating, colony numbers were counted and each colony was picked up and

381 stained with anti-mouse CD45, AA4.1, CD19, B220, and CD11b to identify B-1 and B-2
382 progenitors using flow cytometry.

383

384 ***scRNA-sequencing***

385 E11.5 pre-HSCs, E12.5 and 14.5 FL HSCs were single cell sorted into 96 well plate (1 cell /well).
386 RNA were extracted from each well and converted into cDNA using SAMRT-Seq Single cell kit
387 (Takara). DNA library was made and sequenced at Single Cell Genomic Core at the Baylor
388 College of Medicine. Briefly, following cDNA synthesis, Nextera XT DNA library preparation kit
389 (Illumina) was used to prepare library. 120pg of cDNA was simultaneously fragmented and tagged
390 with adapter sequences by transposome. The product was then amplified using 12 cycles of PCR
391 and purified. Final library was sequenced using Illumina Novaseq 600.

392

393 ***Bioinformatics analysis of scRNA-sequencing***

394 The quality of all sequenced samples was analyzed using FastQC. Raw reads were aligned to
395 the GRCm38 reference genome using STAR with default parameters. The expression count
396 matrix was generated using htseq-count. We filtered genes whose read counts less than 10 and
397 cells that were less than 2000 genes. Read counts were normalized using DEseq2 with default
398 parameters. The normalized matrix was clustered by SC3. We chose K=4 for SC3 as the best
399 represented the heterogeneity in our dataset. Marker genes in each cluster were filtered by the
400 area under the ROC curve (auROC) > 0.85 and the adjusted p-values < 0.01. Trajectory and
401 pseudotime analysis were performed by monocle2 package with default parameters.

402

403 PCA analysis was performed using scikit-learn software package (<https://scikit-learn.org/stable/>).
404 RNA Velocity analysis was performed according to the original article^{31, 32}. Unspliced pre-mRNA
405 counts and mature spliced mRNA counts for each cell were computed from the BAM files
406 generated above., then RNA velocity was computed using scVelo software with default

407 parameters. The result was visualized onto the PCA plot based on the expression profile of mature
408 spliced mRNA for each cell. Each arrow represents a direction of a cell transition based on the
409 RNA Velocity.

410

411 ***Statistical analysis***

412 Non-parametric student-t test was used for statistical analysis.

413

414 **Figure Legends**

415 **Figure 1. B-1a, MPP, and other lymphoid cells arise independently of HSCs and persist into**
416 **adult.**

417 (A) TAM was injected once at E14.5 or P2 into *iFgd5* mice to label HSCs. Tomato⁺ blood cells in
418 the BM, spleen, and peritoneal cavity were examined at different time points after birth. (B) The
419 relative Tomato% ratios of MPP, Follicular (FO) B cells, and B-1a cells to HSCs are shown. TAM
420 was injected to *iFgd5* mice at E14.5 or P2 and mice were examined more than 300 days after
421 birth (n=3-5). (C) TAM was injected into *iCdh5* pregnant mice at E11.5. Tomato⁺ HSPCs were
422 examined at different time points such as E15.5 and after birth. (D) The relative Tomato % ratio
423 of MPPs to LT-HSCs in E15.5 FL when ECs were labeled at E11.5 (n=4). (E) The relative
424 Tomato% ratios of MPPs, splenic FO, and peritoneal B-1a cells to LT-HSCs at different time points
425 (P0-5, days 60-90, days 300<, n=3-6 at each time point). ND: not done. (F) TAM was injected into
426 *iCdh5* pregnant mice at E7.5 and Tomato⁺ HSPCs were examined at different time points such
427 as E15.5 and after birth. (G) The relative Tomato% ratio of each target cell population to LT-HSCs
428 in E15.5 FL, when ECs were labeled at E7.5 (n=6). (H) The relative Tomato% ratio of MPPs to
429 LT-HSCs in the FL and post-natal BM at different time points (P0-5, days 60-90, days 300<, n=3-
430 5). The relative Tomato% ratios of HSPCs and B cell subsets to LT-HSCs at >300 days after birth
431 when TAM was injected at E7.5 (I), E8.5 (J), and E10.5 (K). N=3-7 for each TAM injection. BM:
432 bone marrow, SPL: spleen, PW: peritoneal wash.

433

434 **Figure 2. scRNA-seq analysis showed HSC and B-lymphoid signatures in of E11.5 pre-**
435 **HSCs and E12&14 FL HSCs.**

436 (A) Dimensionality reduction of scRNA-seq data using PCA colored by cell type. E11A, E11.5
437 AGM pre-HSC, E11Y, E11.5 YS pre-HSC, E12F, E12.5 FL HSC, E14F, E14.5 FL HSCs. (B) SC3
438 consensus matrix predicted 4 clusters. (C) A heat map depicting the expression of HSC, B, T,
439 and ILC related genes in E11 AGM&YS pre-HSC populations and E12.5&14.5 FL HSCs. The red,

440 blue, and yellow intensities indicate high, low, and intermediate expression levels, respectively.
441 (D) Velocity analysis of scRNA-seq of E11.5 pre-HSC and E12.5 &14.5 HSCs. Small arrows show
442 the direction of the velocity of single cells. (E) Heat map of gene expressions detected in right and
443 left directions in the velocity analysis, which were applied to gene expressions in the BM HSPC
444 and B-progenitors using the database at ImmGen (<https://www.immgen.org/>).

445

446 **Figure 3. LT-HSCs, MPPs, and B-1 repopulating cells arise independently from CD144⁺c-**
447 **kit⁺EPCR⁺ cells in E11.5 AGM region.**

448 Five to fifty pre-HSCs from E11.5 AGM region were injected into sublethally irradiated NSG
449 neonates. (A) CD45.2⁺ donor cell % in the peripheral blood of the recipient mice 4-6 weeks after
450 transplantation. Donor cells % and their composition within the lymphoid subsets in the peritoneal
451 cells (B), spleen (C), and BM (D) are depicted. The donor-derived cell lineages in the recipient
452 PB during the time course of mouse #2 (E, HSC-engrafted), mouse #9 (I, MPP-engrafted), and
453 #12 (K, B-1 and B-2 cell-engrafted). (H) The % of donor-derived lineages in the recipient BM of
454 mouse #6-10 are depicted. Although the donor cell % was low, multi-lineage repopulation was
455 observed in the recipient BM. The representative FACS plots for donor LSK cells in the first (F,
456 mouse #2 and J, mouse #9) and secondary recipient BM (G).

457

458 **Figure 4. The current and proposed models for developmental hematopoiesis in the mouse**
459 **embryo based on the lineage tracing studies**

460 (A) The summary of the results from HSC- and EC- lineage tracing studies. While HSC-lineage
461 tracing does not label HSC-independent blood lineages (left), EC-lineage tracing labels blood
462 cells with different percentages depending on the timing when those blood cells are produced
463 from ECs (right). EC-labeling at E7.5 marked more HSC-independent blood cell types than HSCs.
464 (B) The current classical hematopoiesis model during fetus. Hemogenic ECs produce EMP,
465 possibly lymphoid progenitors (not indicated), and HSCs. These EMPs and HSCs seed the fetal

466 liver where EMPs provide mature definitive erythroid and myeloid cells and HSC-derived
467 hematopoiesis start while HSC self-renew and expand at the same time. (C) Our working model
468 proposing EC-derived multiple waves of fetal hematopoiesis. Almost all hematopoietic progenitors
469 including EMP, MPP, and B-1 progenitors are produced from hemogenic ECs during E7.5-10.5
470 independently of HSCs. HSC production is the final wave of EC-derived hematopoiesis. These
471 progenitors and HSCs seed the fetal liver and then bone marrow before birth. While HSCs mainly
472 self-renew and expand in the fetal liver, EC-derived (HSC-independent) blood progenitors
473 maintain hematological homeostasis and provide mature blood cell subsets until HSC-derived
474 progenitors replace them in postnatal life. However, peritoneal B-1a cells are not replaced by
475 HSC-derived progenitors and maintain themselves for life.

476 **References**

- 477 1. Chen MJ, Yokomizo T, Zeigler BM, Dzierzak E, Speck NA. Runx1 is required for the
478 endothelial to haematopoietic cell transition but not thereafter. *Nature* **457**, 887-891 (2009).
479
- 480 2. Zovein AC, *et al.* Fate tracing reveals the endothelial origin of hematopoietic stem cells.
481 *Cell Stem Cell* **3**, 625-636 (2008).
482
- 483 3. Tober J, Yzaguirre AD, Piwarzyk E, Speck NA. Distinct temporal requirements for Runx1
484 in hematopoietic progenitors and stem cells. *Development* **140**, 3765-3776 (2013).
485
- 486 4. Dzierzak E, Bigas A. Blood Development: Hematopoietic Stem Cell Dependence and
487 Independence. *Cell Stem Cell* **22**, 639-651 (2018).
488
- 489 5. Ganuza M, Hall T, Finkelstein D, Chabot A, Kang G, McKinney-Freeman S. Lifelong
490 haematopoiesis is established by hundreds of precursors throughout mammalian
491 ontogeny. *Nat Cell Biol* **19**, 1153-1163 (2017).
492
- 493 6. Cumano A, Dieterlen-Lievre F, Godin I. Lymphoid potential, probed before circulation in
494 mouse, is restricted to caudal intraembryonic splanchnopleura. *Cell* **86**, 907-916 (1996).
495
- 496 7. Nishikawa SI, *et al.* In vitro generation of lymphohematopoietic cells from endothelial cells
497 purified from murine embryos. *Immunity* **8**, 761-769 (1998).
498
- 499 8. Yokota T, *et al.* Tracing the first waves of lymphopoiesis in mice. *Development* **133**, 2041-
500 2051 (2006).
501
- 502 9. Yoshimoto M, *et al.* Embryonic day 9 yolk sac and intra-embryonic hemogenic
503 endothelium independently generate a B-1 and marginal zone progenitor lacking B-2
504 potential. *Proc Natl Acad Sci U S A* **108**, 1468-1473 (2011).
505
- 506 10. Hardy RR, Hayakawa K. A developmental switch in B lymphopoiesis. *Proc Natl Acad Sci*
507 *U S A* **88**, 11550-11554 (1991).
508
- 509 11. Kristiansen TA, *et al.* Cellular Barcoding Links B-1a B Cell Potential to a Fetal
510 Hematopoietic Stem Cell State at the Single-Cell Level. *Immunity* **45**, 346-357 (2016).
511
- 512 12. Beaudin AE, *et al.* A Transient Developmental Hematopoietic Stem Cell Gives Rise to
513 Innate-like B and T Cells. *Cell Stem Cell* **19**, 768-783 (2016).
514

- 515 13. Ghosn EE, *et al.* Fetal Hematopoietic Stem Cell Transplantation Fails to Fully Regenerate
516 the B-Lymphocyte Compartment. *Stem Cell Reports* **6**, 137-149 (2016).
517
- 518 14. Kobayashi M, *et al.* Hemogenic Endothelial Cells Can Transition to Hematopoietic Stem
519 Cells through a B-1 Lymphocyte-Biased State during Maturation in the Mouse Embryo.
520 *Stem Cell Reports* **13**, 21-30 (2019).
521
- 522 15. Gazit R, *et al.* Fgd5 identifies hematopoietic stem cells in the murine bone marrow. *J Exp*
523 *Med* **211**, 1315-1331 (2014).
524
- 525 16. Sawen P, *et al.* Murine HSCs contribute actively to native hematopoiesis but with reduced
526 differentiation capacity upon aging. *Elife* **7**, (2018).
527
- 528 17. Hadland B, Yoshimoto M. Many layers of embryonic hematopoiesis: new insights into B
529 cell ontogeny and the origin of hematopoietic stem cells. *Exp Hematol* **60**, 1-9 (2018).
530
- 531 18. Dignum T, *et al.* Multipotent progenitors and hematopoietic stem cells arise independently
532 from hemogenic endothelium in the mouse embryo. *Cell Rep* **36**, 109675 (2021).
533
- 534 19. Wang Y, *et al.* Ephrin-B2 controls VEGF-induced angiogenesis and lymphangiogenesis.
535 *Nature* **465**, 483-486 (2010).
536
- 537 20. Gentek R, *et al.* Hemogenic Endothelial Fate Mapping Reveals Dual Developmental Origin
538 of Mast Cells. *Immunity* **48**, 1160-1171 e1165 (2018).
539
- 540 21. Ema H, Nakauchi H. Expansion of hematopoietic stem cells in the developing liver of a
541 mouse embryo. *Blood* **95**, 2284-2288 (2000).
542
- 543 22. Rybtsov S, Ivanovs A, Zhao S, Medvinsky A. Concealed expansion of immature
544 precursors underpins acute burst of adult HSC activity in foetal liver. *Development* **143**,
545 1284-1289 (2016).
546
- 547 23. Busch K, *et al.* Fundamental properties of unperturbed haematopoiesis from stem cells in
548 vivo. *Nature* **518**, 542-546 (2015).
549
- 550 24. Rybtsov S, *et al.* Hierarchical organization and early hematopoietic specification of the
551 developing HSC lineage in the AGM region. *J Exp Med* **208**, 1305-1315 (2011).
552

- 553 25. Souilhoul C, *et al.* Developing HSCs become Notch independent by the end of maturation
554 in the AGM region. *Blood* **128**, 1567-1577 (2016).
555
- 556 26. Yuan J, Nguyen CK, Liu X, Kanellopoulou C, Muljo SA. Lin28b reprograms adult bone
557 marrow hematopoietic progenitors to mediate fetal-like lymphopoiesis. *Science* **335**, 1195-
558 1200 (2012).
559
- 560 27. Ghosn E, Yoshimoto M, Nakauchi H, Weissman IL, Herzenberg LA. Hematopoietic stem
561 cell-independent hematopoiesis and the origins of innate-like B lymphocytes.
562 *Development* **146**, (2019).
563
- 564 28. DiMartino JF, *et al.* The Hox cofactor and proto-oncogene Pbx1 is required for
565 maintenance of definitive hematopoiesis in the fetal liver. *Blood* **98**, 618-626 (2001).
566
- 567 29. Sanyal M, *et al.* B-cell development fails in the absence of the Pbx1 proto-oncogene.
568 *Blood* **109**, 4191-4199 (2007).
569
- 570 30. Ficara F, Murphy MJ, Lin M, Cleary ML. Pbx1 regulates self-renewal of long-term
571 hematopoietic stem cells by maintaining their quiescence. *Cell Stem Cell* **2**, 484-496
572 (2008).
573
- 574 31. La Manno G, *et al.* RNA velocity of single cells. *Nature* **560**, 494-498 (2018).
575
- 576 32. Bergen V, Lange M, Peidli S, Wolf FA, Theis FJ. Generalizing RNA velocity to transient
577 cell states through dynamical modeling. *Nature biotechnology* **38**, 1408-1414 (2020).
578
- 579 33. Sun J, *et al.* Clonal dynamics of native haematopoiesis. *Nature* **514**, 322-327 (2014).
580
- 581 34. Upadhaya S, *et al.* Kinetics of adult hematopoietic stem cell differentiation in vivo. *J Exp*
582 *Med* **215**, 2815-2832 (2018).
583
- 584 35. Zhang Y, *et al.* Mds1(CreERT2), an inducible Cre allele specific to adult-repopulating
585 hematopoietic stem cells. *Cell Rep* **36**, 109562 (2021).
586
- 587 36. Ulloa BA, *et al.* Definitive hematopoietic stem cells minimally contribute to embryonic
588 hematopoiesis. *Cell Rep* **36**, 109703 (2021).
589
- 590 37. Soares-da-Silva F, *et al.* Yolk sac, but not hematopoietic stem cell-derived progenitors,
591 sustain erythropoiesis throughout murine embryonic life. *J Exp Med* **218**, (2021).

592
593

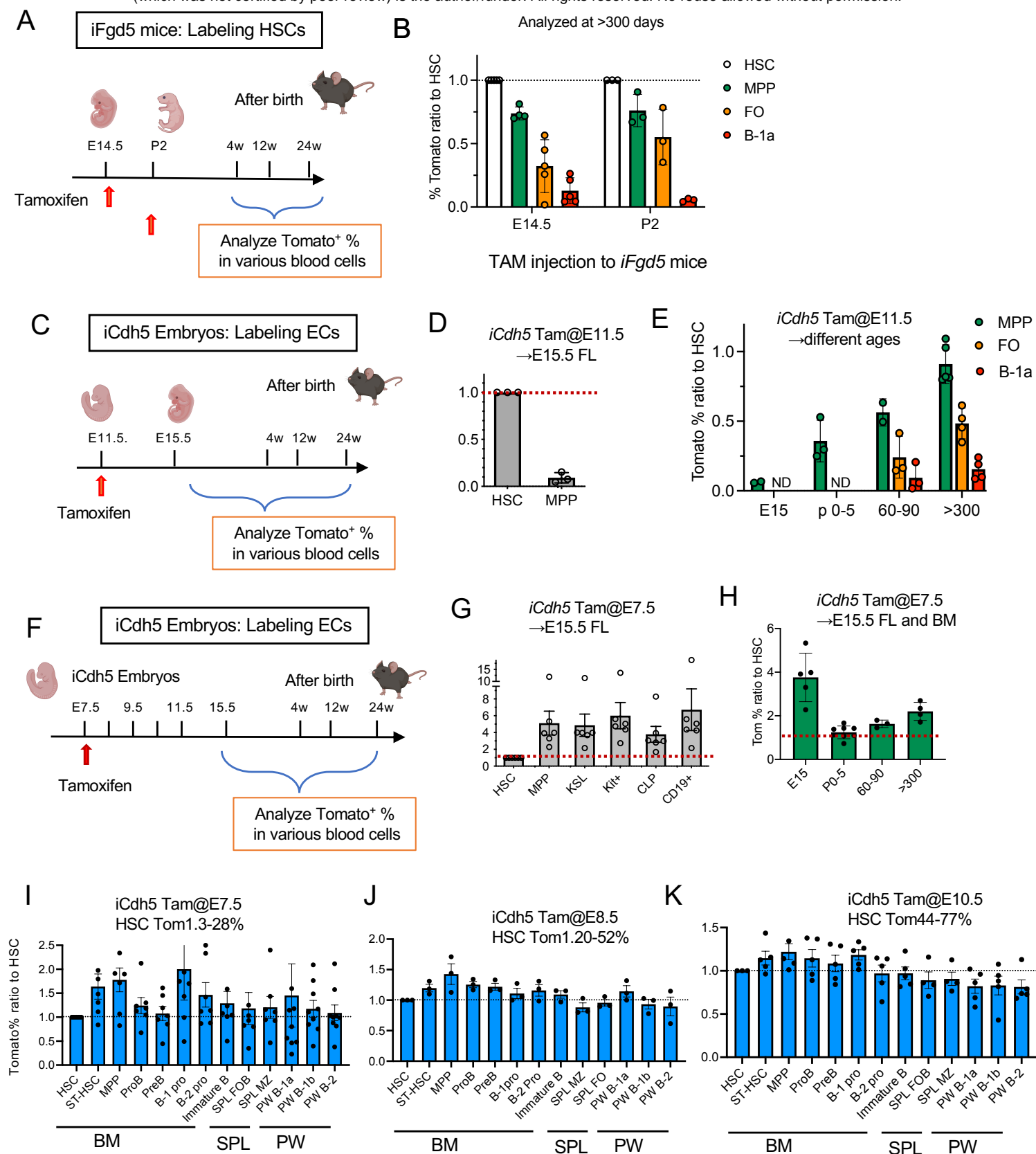


Figure 1

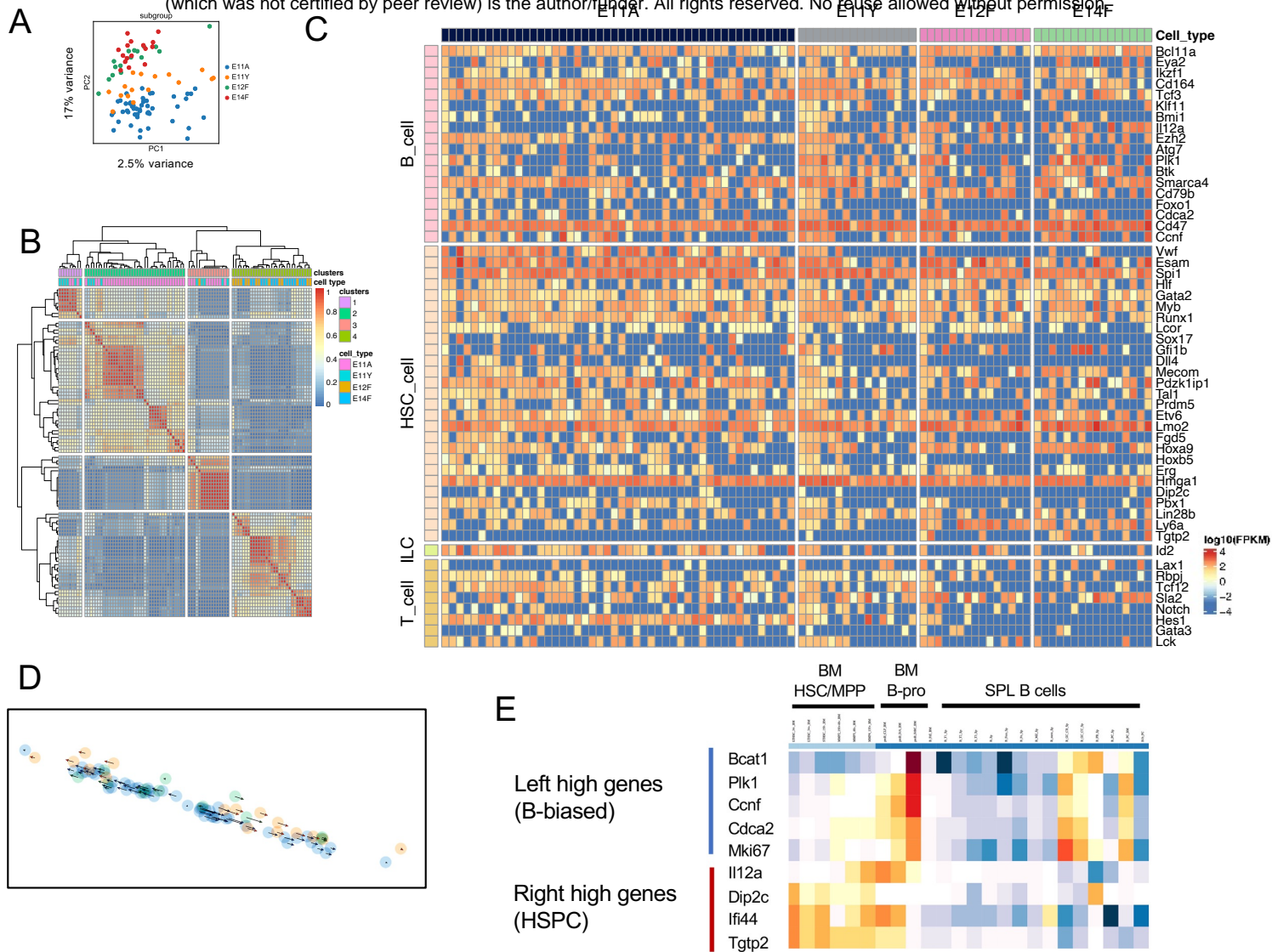


Figure 2

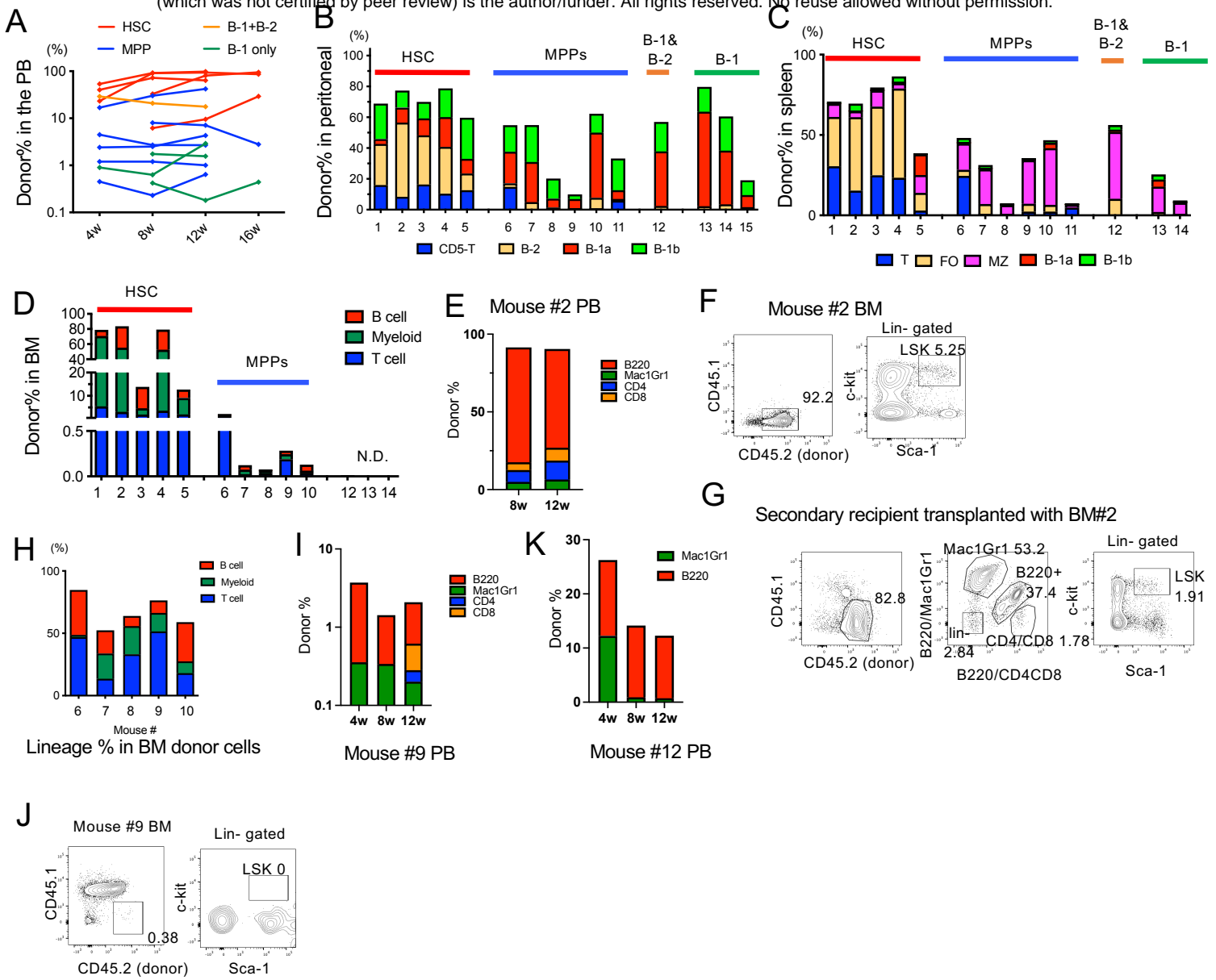


Figure 3

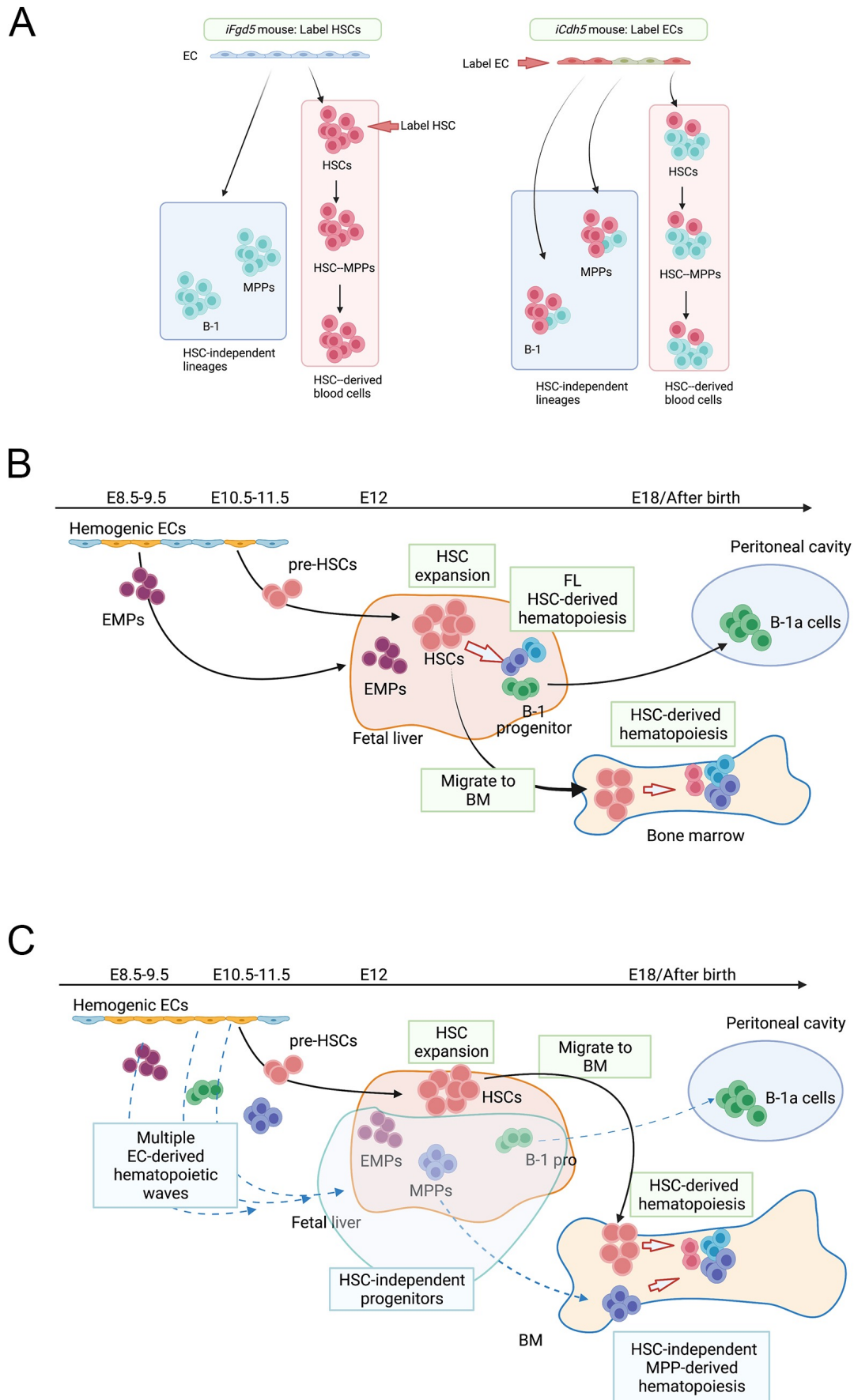


Figure. 4